

Cytocompatibility of direct water synthesized cadmium selenide quantum dots in colo-205 cells

Marcos R. Rodriguez-Torres · Christian Velez · Beatriz Zayas ·
Osvaldo Rivera · Zikri Arslan · Maxine N. Gonzalez-Vega · Daysi Diaz-Diestra ·
Juan Beltran-Huarac · Gerardo Morell · Oliva M. Primera-Pedrozo

Received: 3 March 2015 / Accepted: 3 June 2015
© Springer Science+Business Media Dordrecht 2015

Abstract Cadmium selenide quantum dots (CdSe QDs), inorganic semiconducting nanocrystals, are alluring increased attraction due to their highly refined chemistry, availability, and super tunable optical properties suitable for many applications in different research areas, such as photovoltaics, light-emitting devices, environmental sciences, and nanomedicine. Specifically, they are being widely used in bio-imaging in contrast to organic dyes due to their high brightness and improved photo-stability, and their ability to tune their absorption and emission spectra upon changing the crystal size. The production of CdSe QDs is mostly assisted by trioctylphosphine oxide compound, which acts as solvent or solubilizing agent and renders the QDs soluble in organic compounds (such as toluene, chloroform, and hexane) that are highly toxic. To circumvent the toxicity-related factor in CdSe QDs, we report the synthesis of CdSe QDs capped with

thioglycolic acid (TGA) in an aqueous medium, and their biocompatibility in colo-205 cancer cells. In this study, the $[Cd^{2+}]/[TGA]$ ratio was adjusted to 11:1 and the Se concentration (10 and 15 mM) was monitored in order to evaluate its influence on the optical properties and cytocompatibility. QDs resulted to be quite stable in water (after purification) and RPMI cell medium and no precipitation was observed for long contact times, making them appealing for in vitro experiments. The spectroscopy analysis, advanced electron microscopy, and X-ray diffractometry studies indicate that the final products were successfully formed exhibiting an improved optical response. Colo-205 cells being exposed to different concentrations of TGA-capped CdSe QDs for 12, 24, and 48 h with doses ranging from 0.5 to 2.0 mM show high tolerance reaching cell viabilities as high as 93 %. No evidence of cellular apoptotic pathways was observed as pointed out by our

M. R. Rodriguez-Torres · O. Rivera ·
M. N. Gonzalez-Vega · O. M. Primera-Pedrozo (✉)
Nanomaterials Science Laboratory, School of Science and
Technology, Universidad Metropolitana, San Juan, PR,
USA
e-mail: oprimeral@suagm.edu

C. Velez · B. Zayas
ChemTox Laboratory, School of Environmental Affairs,
Universidad Metropolitana, San Juan, PR, USA

Z. Arslan
Department of Chemistry, Jackson State University,
Jackson, MS, USA

D. Diaz-Diestra · J. Beltran-Huarac · G. Morell
Molecular Science Research Center, University of Puerto
Rico, San Juan, PR 00926, USA

D. Diaz-Diestra
Department of Chemistry, University of Puerto Rico,
San Juan, PR 00936, USA

J. Beltran-Huarac · G. Morell
Department of Physics, University of Puerto Rico,
San Juan, PR 00936, USA

Annexin V assays at higher concentrations. Moreover, confocal microscopy analysis conducted to evaluate the intracellular uptake of TGA-CdSe QDs reveal that the TGA-CdSe QDs were uniformly distributed within the cytosolic side of cell membranes. Our results also suggest that under controlled conditions, direct water-soluble TGA-CdSe QDs can be potentially employed for bio-imaging colo-205 cancer cells with minimal adverse effects.

Keywords CdSe QDs · Water · Cell viability · Colo-205 · Annexin V · Bio-imaging · Biomedicine

Introduction

In recent years, many efforts have been made to synthesize cadmium selenide (CdSe) metal-based quantum dots (QDs) for potential applications in nanomedicine due to their size-dependent fluorescence, anti-photobleaching, long-term imaging, high brightness, tunable absorption and emission, and rapid detection, when contrasted to the conventional organic dyes (Walling et al. 2009; Jaiswal et al. 2003; Xue et al. 2011; Jamieson et al. 2007; Yu et al. 2006). Nonetheless, CdSe QDs present a significant disadvantage when used as bio-imaging agent since they suffer instability and are vulnerable to the release of Cd²⁺ ions into biological settings (Derfus et al. 2004), which is critical to evaluate their biocompatibility in human cells. Worse yet, it has been reported that such ions tend to be accumulated into the nervous system, kidneys, and specifically in the liver (Arslan et al. 2011). To tackle this drawback, some alternative stabilizing surface coating approaches to both substantially reduce the leeching of Cd²⁺ ions and effectively protect the core materials from oxidation, as well as new synthetic procedures able to control the [Metal:Se:ligand] ratios without causing any optical detriment, have been proposed (Arslan et al. 2011; Primera-Pedrozo et al. 2012; Xue et al. 2011). CdSe QDs can be in fact capped with different ligands or biomolecules, such as glutathione (GSH) or thioglycolic acid (TGA), thus relatively reducing their cytotoxicity (Aldeek et al. 2008; Gaponik et al. 2002). Parallely, it has been demonstrated that their bioconjugation through folic acid endows QDs with further stability and biocompatibility (Xue et al. 2011).

Nevertheless, recent studies reveal that CdSe QDs still cause irreversible cellular damage and eventually cellular death by apoptosis (Chan et al. 2006; Fang et al. 2012). News methods to synthesize CdSe QDs directly in water with an efficient capping ligand at a suitable [Metal:Se:ligand] ratio capable to be tolerated by human cells and to be used as potential nano-probes for detecting cancer cells are still a challenge.

Among the most common cancer types, colorectal cancer is of considerable national interest due to the high mortality rate that it causes per year, with an estimated burden of ~21 cases out of 100,000 in the US (Rim et al. 2009). Although many techniques, such as fluorescence microscopy, endoscopy, and NIR-light-induced surface-enhanced Raman scattering have appeared in literature to detect colorectal cancer cells, optical-sectioned fluorescence microscopy has demonstrated in practice to be more efficient to detect and analyze live cells due to its improved axial resolution, super resolution, and low-temperature operability (Dailey et al. 2006). In this line, recent reports have validated that CdSe/CdS/ZnS QDs conjugated with antibodies can detect cancerous tissues inside live animals upon spraying QDs bioconjugates in the colon section, which allowed for a rapid and multiplex cancer diagnosis (Park et al. 2014). Similar findings on the cytotoxic effects of CdSe QDs have been reported working with different cellular lines, ranging from human cells (including neuroblastoma, osteoblast, hepatocyte line, and vascular endothelial) to bacteria such as *E. coli* (Jayagopal et al. 2007; Lu et al. 2006; Yan et al. 2011). However, no study focusing on the cytocompatibility or cytotoxic effect of TGA-capped CdSe QDs in colo-205 cancer cells has been reported to date. We herein report the optimized direct water synthesis and characterization of CdSe QDs using TGA as a capping agent varying the concentrations of selenium (Se IV), and the correlated study of their cytotoxicity in colo-205 cancer cells. The intracellular uptake study and apoptosis Annexin V assay analysis of cells exposed to TGA-capped CdSe QDs are also discussed.

Materials and methods

Reagents and solutions

Deionized water (18.2 MΩ) was obtained from an Aries Filter Works Reverse Osmosis System.

Cadmium chloride (CdCl_2 , 99.99 %, trace metals basis), thioglycolic acid (TGA, ≥ 98 %), sodium borohydride (NaBH_4 , ≥ 98.0 %) and selenium powder (99.999 %, metal basis) were obtained from Alfa Aesar. Dimethyl sulfoxide (DMSO, 99.9 %) was purchased from VWR. Nitric Acid (HNO_3 , 67–70 %, trace metal grade, OmniTrace) and HCl (trace metal grade, 34–37 %, Fisher Scientific) were used for the selenium stock solution preparation. A 3:1 solution of *aqua regia* was prepared using HCl (37 %, Sigma-Aldrich) and nitric acid (65 %, J.T. Baker), respectively. A 5.0 N sodium hydroxide (NaOH) solution was prepared by diluting NaOH (10.0 N standardized solution), purchased from Alfa Aesar. The solutions in each synthetic protocol were purged with 99.99 % pure nitrogen gas obtained from Linde Gas Corporation. Selenium stock solution was prepared by dissolving 4.0 g of selenium powder in 8.0 mL of concentrated HNO_3 in a 125-mL Erlenmeyer flask. The solution was heated in order to evaporate the excess of acid. One hundred (100 mL) of 10 % v/v HCl was then added to reduce Se(VI) to Se(IV). The final concentration of the stock solution was adjusted to 0.5 M.

Synthesis of CdSe QDs at different Cd/Se ratios

The synthesis was performed following our previous synthetic methodology (Arslan et al. 2011; Primera-Pedrozo et al. 2012) with some modifications. Briefly, the glassware was roughly cleaned with *aqua regia* for 12 h and then rinsed thoroughly with ultra-high pure water (dH_2O). An aqueous solution of Se (IV) was used as the selenium source. A cadmium chloride solution was used as the cadmium source. 500 μL of CdCl_2 was added to 250 mL of dH_2O under constant stirring in a three-neck round flask (flask 1). Concentrated TGA (500 μL) was then added to the solution, which turned turbid. The pH level was adjusted to ~ 9.5 by adding a solution of NaOH 5.0 N. After reaching the desired pH value, the solution turned clear, indicating that the cadmium and the ligand dissolved completely. In a separate three-neck round flask (flask 2), a Se (IV) solution was added. Different concentrations of selenium (10 and 15 mM) were used for each synthesis. Flask 2 was connected to flask 1 using a Teflon tubing. Both flasks were then purged with pure nitrogen gas for 30 min in order to remove all the surrounding oxygen. Ten milliliter (10 mL) of

freshly prepared 10 % w/v NaBH_4 (in 0.1 % w/v NaOH) was added to flask 2 using a plastic syringe, whereas the N_2 flow was kept on in order to generate hydrogen selenide gas. The solution was added dropwise in order to favor the formation of monodispersed QDs. The color change in flask 1, as the NaBH_4 solution was added, indicated that the formation of QDs in flask 1 started almost instantly. After 20 min of reaction, the N_2 flow was shut off and flask 1 was left under reflux overnight. As for the time interval measures, the synthesis was stopped every 20 min of reflux process in order to obtain smaller QDs.

Purification

DMSO was used as a solvent in the purification process of CdSe QDs. The temperature of both the QDs and DMSO was decreased using an ice bath for 10 min. One hundred milliliter (100 mL) of QDs was distributed in five 50-mL polystyrene centrifuge tubes (20 mL per tube), then 20 mL of DMSO was added to each tube and they were kept in the ice bath for 10 min. The products were then centrifuged in an IEC FL40R Centrifuge (Thermo Electron Corporation) for 30 min at 6000 rpm with a temperature of 4 °C. The supernatant was carefully removed from each tube and the pellets were re-dispersed into 1 mL of dH_2O . All the tube-contained solutions were then combined in a 15-mL polystyrene centrifuge tube. The concentration of solutions was increased 10 times from the stock solution by adding dH_2O up to a final volume of 10 mL (100 mL of QDs to 10 mL).

Determination of cadmium and selenium concentration by ICP-MS

The concentrations and ratios of cadmium/selenium were determined using a Varian 820MS ICP-MS instrument (Varian, Australia). CdSe QDs suspensions were purified as described on the previous section. One milliliter (1 mL) of concentrated HNO_3 was added to 100 μL of the CdSe QDs ($\times 10$) in a 15-mL tube. The solution was heated up to 100 °C for 10 min, and then exposed to a fume hood for 24 h. The final volume was fixed at 10 mL with 5 % v/v HNO_3 . Quantification process was performed using ^{206}Cd and ^{208}Cd isotopes for Cd, and ^{78}Se and ^{82}Se isotopes for Se. The concentrations for Cd and Se are reported as the average standard deviation of both isotopes.

Characterization

The absorbance spectra of the CdSe QDs were obtained using a DR 5000 UV–Vis spectrophotometer. The stock solutions were diluted 20 times in dH₂O in optically transparent cuvettes. The fluorescence spectra were obtained using a Varian Cary Eclipse Fluorescence Spectrophotometer. The diffraction patterns were collected using a Rigaku Miniflex X-ray Powder Diffractometer in 2θ configuration ranging from 20° to 80° with a scanning speed of 0.1° min⁻¹ per one scan. FT-IR spectra were recorded using an IRAffinity-1 Fourier transform infrared spectrophotometer (Shimadzu) in the 100–4000 cm⁻¹ range. XRD and FT-IR measurements were conducted using powdered QDs. The morphology and size distribution were analyzed using a Carl Zeiss Leo 922 transmission electron microscope (TEM). TEM samples were prepared by dripping a stable suspension of TGA-CdSe QDs onto a lacey carbon Cu-supported grid (01895-F Ted Pella, Inc.). Bright-field TEM images at different magnifications were acquired under a continuous accelerating voltage of 200 kV.

Cytotoxic experiments

QDs stability in cell culture medium (RPMI 1640)

It is of utmost importance that the QDs remain stable under different conditions, as they are exposed to temperature and medium changes. In order to determine their stability, QDs at 0.5, 1.0, and 1.0 mM were dispersed in RPMI-1640 culture medium monitoring their UV–Vis absorbance and fluorescence. Afterward, they were exposed to cell culture conditions (37°, 5 % CO₂) for 48 h. Their corresponding UV–Vis and fluorescence spectra were analyzed before and after exposure, and analyzed again in order to detect any optical change.

Cell culture

The cellular line used in this study was the colo-205 human colorectal adenocarcinoma (ATCC CCL-222). Cells were maintained in RPMI 1640 (ATCC, Manassas VA) containing 10 % fetal bovine serum (ATCC). Cells were maintained at 37 °C with humidified atmosphere of 95 % air and 5 % CO₂. Cells at a density of 2.5×10^5 cells/mL were cultured in 12.5-cm²

flasks in duplicate and incubated for 4 h to allow cells to adhere in a normal fashion before being exposed to the testing compounds. Cell cultures contained a total volume of 5 mL including modified RPMI 1640 medium (10 % FBS) and the CdSe QDs.

QD Biocompatibility in colo-205 cells

Cell viability over a period of 48 h was evaluated. Two experimental groups were prepared; cells were divided and seeded in two 50-mL centrifuge tubes for a total of 5×10^6 cells. Cells in RPMI-1640 medium only were used as the control group, while the other experimental group was exposed to 0.5, 1.0, and 2.0 mM of CdSe QDs. Both tubes were kept at the same conditions as the stock culture. Samples of each experimental culture were taken at 12, 24, and 48 h. After fluorescence analysis, cells were stained with trypan blue exclusion and counted using a Countess automated cell counter (Life, technologies, Carlsbad, Ca.) to assess viability. One-way ANOVA and post hoc Tukey tests were also performed using Graph pad program.

Annexin V

Approximately, 1×10^6 cells were treated for 48 h with a QDs concentration of 2 mM. Positive controls were camptothecin at a 10 μM concentration and 2 mM Cd²⁺. After 48 h of exposure, cells were stained with Annexin V conjugate and propidium iodide (Biotium, Hayward, CA) as directed by the manufacturer. QDs were then analyzed using a Nucleo Counter NC3000 (Chemometec, Allerød, Denmark). Experiments were performed using CdSe QDs prepared at 10 and 15 mM of Se (IV).

Cell uptake

Treated cells used for biocompatibility assessment were also used for intracellular uptake determination. Intracellular uptake of TGA-CdSe QDs in colo-205 cells was determined using a fluorescence microscope Zeiss LSM 510 on an Axiovert 200 M microscope. Cells were washed two times and re-dispersed in PBS to remove any excess QDs in suspension. The QDs used were synthesized as explained in the synthesis section; however, they were refluxed each 20 min in order to obtain detectable fluorescence emission.

Results and discussion

Stable TGA-capped CdSe QDs were obtained with no visual evidence of bulk material or precipitation during 6 months after preparation. As discussed in the experimental section, QDs were synthesized directly in water in an oxygen-free environment under reflux process overnight. TGA was used as a stabilizer with a [TGA]/[Cd²⁺] molar ratio of 11:1, and cadmium concentrations were kept constant. In order to study the effects of selenium concentrations on the optical properties, two suspensions were prepared, one at 10 mM of Se(IV) and the other at 15 mM (see inset of Fig. 1). These show the typical red color of CdSe QDs at this particular size regime (Robel et al. 2006). The color change is ascribed to the quantum confinement effects, indicating that the suspensions exhibit different crystal sizes. These results were confirmed by their corresponding absorption spectra displayed in Fig. 1. Two broadband absorption edges were observed at ~ 2.31 eV (535 nm, 10 mM) and ~ 2.24 eV (553 nm, 15 mM), and attributed to the energy transfer of the *s-p* electron-hole pairs in CdSe (Robel et al. 2006). By comparing such spectra to the sizing curve reported by Yu et al. we obtain particle diameters falling in the range of 2.5–4.0 nm (Yu et al. 2003). The fluorescence spectra of both suspensions (see Fig. 2) show the typical emission bands of CdSe QDs centered at 734 nm (10 mM) and 742 nm (15 mM) with a slight upshift (~ 8 nm) in the red

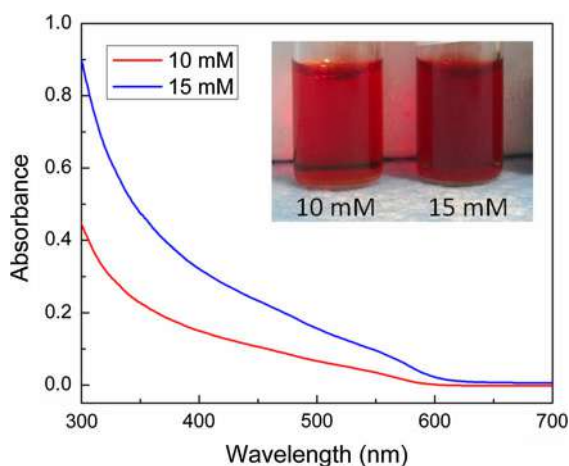


Fig. 1 UV-Vis absorption spectra of TGA-capped CdSe QDs at 10 and 15 mM of Se(IV). Inset shows the corresponding optical images of the solutions diluted 10 times

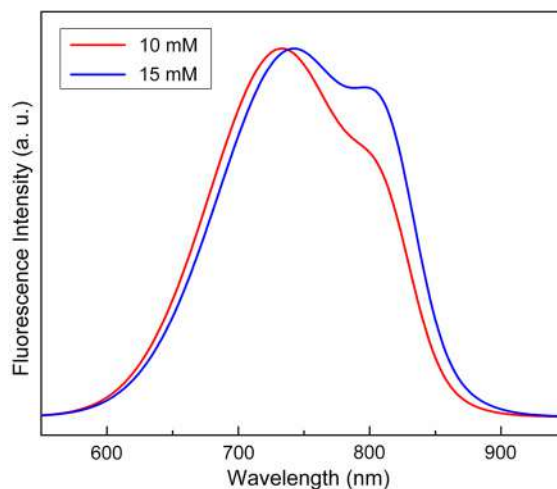


Fig. 2 Fluorescence emission spectra of CdSe QDs at 10 mM (734 nm) and 15 mM (742 nm) of Se(IV) when exposed to 450–500-nm light

emission band, which is associated to the deactivation of the excited electrons from *p*-states to the *s*-states in CdSe (Robel et al. 2006).

The TEM images of QDs are displayed in Fig. 3. Our observations indicate that the TGA-CdSe QDs are well-dispersed, near-spherical, and highly crystalline forming regular clusters. The statistical distributions of the particle size were modeled using standard Gaussian fits (Beltran-Huarac et al. 2013), which reveal that the average sizes of particles are in the range of 2–4 nm for 10 mM and 6–8 nm for 15 mM with FWHM of 1.9 and 1.1 nm, respectively, partially consistent with the optical studies. The relatively uniform dispersion of CdSe QDs in water is correlated to the effective TGA capping process, although certain agglomeration was observed when selenium concentration was increased. Taken altogether, the role of selenium concentrations on the changes in size, absorbance and fluorescence spectra can be explained in terms of the addition of selenium to the solution that combined with unreacted cadmium (supplied by the cadmium chloride source) enable that the already formed CdSe crystals adsorb more Cd and Se, thus increasing significantly their size. This effect was corroborated by the redshift observed in both absorbance and emission spectra of TGA-capped CdSe QDs, and by the TEM analysis.

The structural phase of the QDs was studied by X-ray diffraction. The diffraction peaks depicted in Fig. 4 were indexed to the diffraction planes of

Fig. 3 Bright-field TEM images of TGA-capped CdSe QDs at (a, b) 10 mM and (d, e) 15 mM of Se(IV), and their corresponding (c, f) statistical distributions of particle size peaking at ~ 3 and 8 nm, respectively

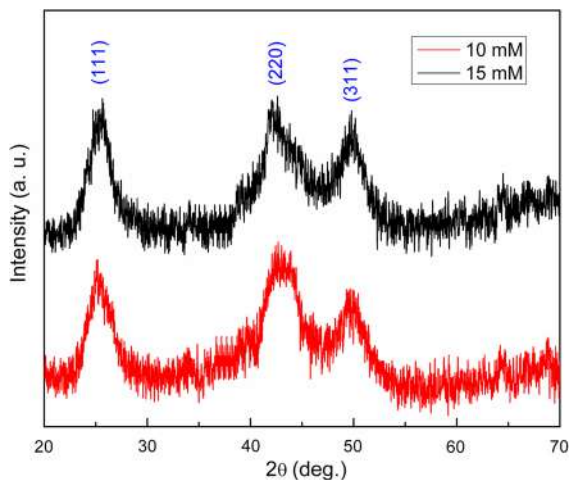
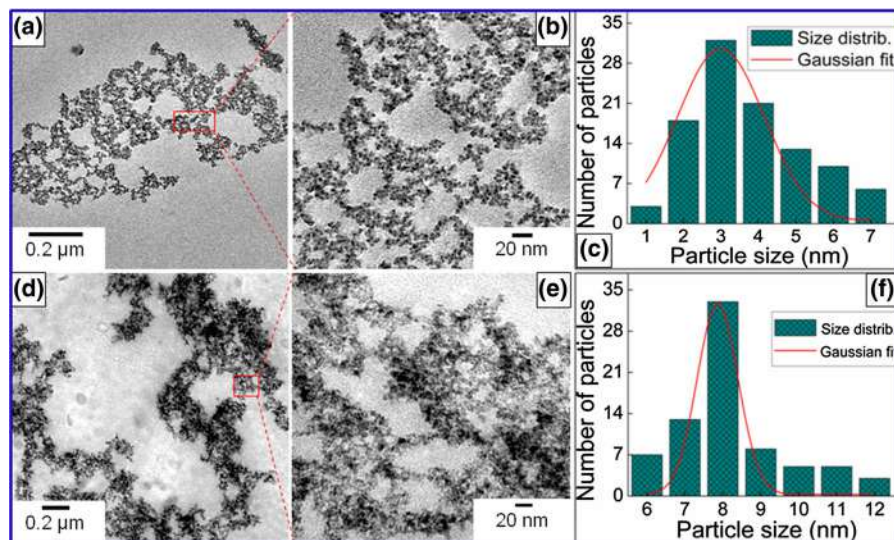


Fig. 4 XRD patterns of powdered CdSe QDs at 10 and 15 mM of Se(IV). No parasitic phases were observed

cubic CdSe phase [(111), (220), and (311)] according to the JCPDS file No. 19-0191 (Zhai et al. 2011). The relatively sharp peaks found and the absence of impurities in the XRD patterns indicates that the CdSe phase is of high crystalline quality and purity. To evaluate the stoichiometric ratios of Cd and Se in purified CdSe QDs, we conducted ICP-MS spectroscopy. The main results are summarized in Table 1. The analysis shows Cd/Se ratios of ~ 1.28 (10 mM) and ~ 1.32 (15 mM) closely compatible with those reported for CdSe (Lewinski et al. 2010).

Table 1 Elemental composition of Cd and Se in purified CdSe QDs extracted from ICP-MS analysis

Se(IV) (mM)	Cd (mM)	Se (mM)	Cd/Se ratio
10	62	48	1.28
15	83	63	1.32

To further confirm the successful bonding of TGA capping ligand onto the QDs surfaces, we conducted FT-IR analysis. The FT-IR spectra of QDs are depicted in Fig. 5. Note that in our synthetic procedure the pH levels were adjusted to 9.3–9.6 to deprotonate the carboxylic end of the TGA, and in turn to reinforce the bonding. TGA possesses S–H bonds that show vibrations modes in the range of 2400–2542 cm^{-1} (Fig. 5, top). However, the spectra of the QDs show that such vibrational modes vanish when TGA-capped CdSe regardless of the Se(IV) volume were used, indicating the successful formation of S–Cd bonds between the ligand and QDs (Jiang and Ju 2007). It was also observed that the characteristic mode of the C=O functional group of TGA was shifted from $\sim 1700 \text{ cm}^{-1}$ to 1560 cm^{-1} for both suspensions (Primera-Pedrozo et al. 2012). No strong OH⁻ vibrations were detected. The presence of carboxylate moieties in the range of 1400–1470 and 1616–1663 cm^{-1} can be assigned to the symmetric $\nu_s(\text{COO}^-)$ and asymmetric $\nu_{as}(\text{COO}^-)$ vibrational modes. The moieties detection is a clear indicator of the successful deprotonation process of the carboxylic acid in TGA. The presence of these bands in the FT-IR

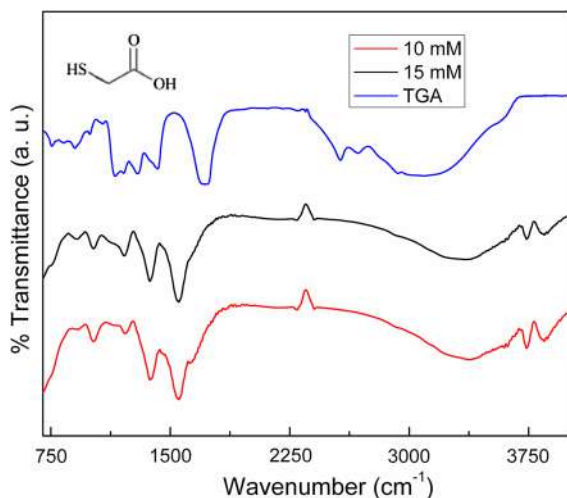


Fig. 5 FT-IR spectra of pure TGA and TGA-capped CdSe QDs at 10 and 15 mM of Se(IV) at room temperature. *Inset* chemical structure of TGA

spectra confirms the existence of carboxylate moieties on the QDs surface, as reported in previous studies on the absorption of carboxylic acids on metal surfaces (Primera-Pedrozo et al. 2012). It was also observed a low-frequency vibrational mode located at 669 cm^{-1} , which was assigned to the C–S stretching mode, further confirming the TGA bonding onto the QDs surface. Additional band assignments observed in CdSe QDs are summarized in Table 2.

For the effective use of nanoparticles and QDs in biomedicine, their stabilities in cell media are of great importance. As previously reported (Kinkeada and Hegmann 2009) the emission and absorption spectra of QDs strongly depend on their dimension at the nanoscale. In the present study, it is shown that TGA-capped CdSe QDs dispersed in water with sizes of 2–4 and 6–8 nm exhibit prominent emission bands peaking at 734 and 742 nm, respectively. Thus, in order to evaluate the optical stability in RPMI media, CdSe QDs at 15 mM (Se) were exposed to RPMI media for 48 h at $37\text{ }^{\circ}\text{C}$ and 5 % CO_2 atmosphere, the same concentrations and conditions used for in vitro experiments. The UV–Vis absorption spectra of CdSe (see Fig. 6) show that QDs are highly stable in the cell culture. From the absorption profile, only a negligible redshift ($\sim 3\text{ nm}$) was observed. Fluorescence emission (Fig. 7a, b) evidences that the CdSe QDs (before and after exposure of RPMI media) remain stable with a slight shift of $\sim 20\text{ nm}$, which can be attributed to

Table 2 Bands assignments of the vibrational modes in purified TGA-capped CdSe QDs obtained from FT-IR spectra

FT-IR spectral region (cm^{-1})	Band assignment
~ 660	C–S
$1400\text{--}1470\text{ cm}^{-1}$	$\nu_s(\text{COO}^-)$
1560 cm^{-1}	C = O
$1616\text{--}1663\text{ cm}^{-1}$	$\nu_{as}(\text{COO}^-)$
$2400\text{--}2542\text{ cm}^{-1}$	S–H ^a

^a This band is only present in pure TGA

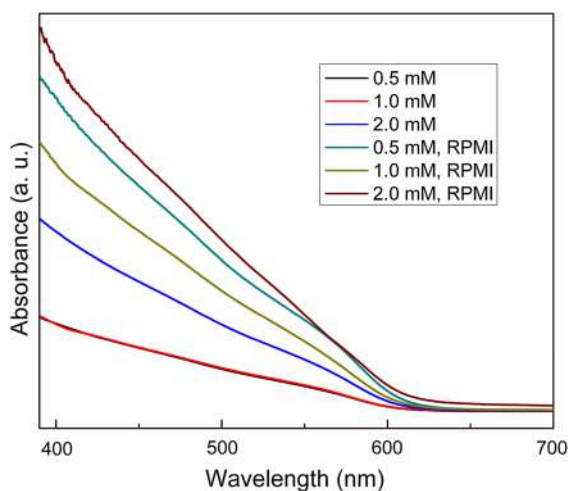


Fig. 6 UV–Vis absorption spectra before and after exposure with RPMI media showing the stability of CdSe QDs at 15 mM Se in RPMI cell media for 48 h at $37\text{ }^{\circ}\text{C}$ under humidified atmosphere conditions of 95 % air and 5 % CO_2

the interaction of the QDs with the surrounding media (RPMI). These results support the excellent optical stability that the QDs possess before and after purification and exposure to cell media, which is vital for biological applications. No apparent aggregation was observed after 48 h in cell media that may influence the QDs–cell interactions and uptake process.

The cytotoxic effect of TGA-capped CdSe QDs was assessed by viability assay exposing colo-205 cells to QDs (12, 24 and 48 h) through trypan blue staining. The cell viability results for CdSe QDs at 10 and 15 mM of Se(IV) are depicted in Fig. 8. They indicate that the cancer cells can tolerate the QDs (from 0.5 to 2.0 mM) with high values of viability even after 48 h of contact. Specifically, the control samples presented an average of 91.7 % of viable

Fig. 7 Fluorescence emission spectra of CdSe QDs at 15 mM Se before (a) and after (b) exposure with RPMI media, and excited with 450–500-nm light

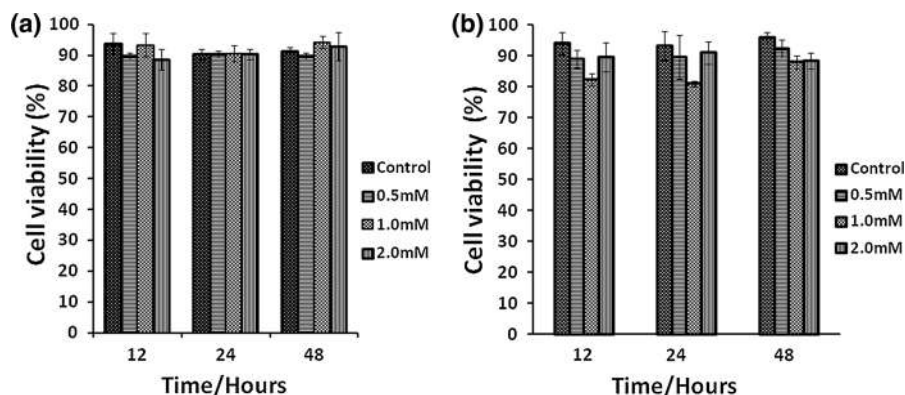
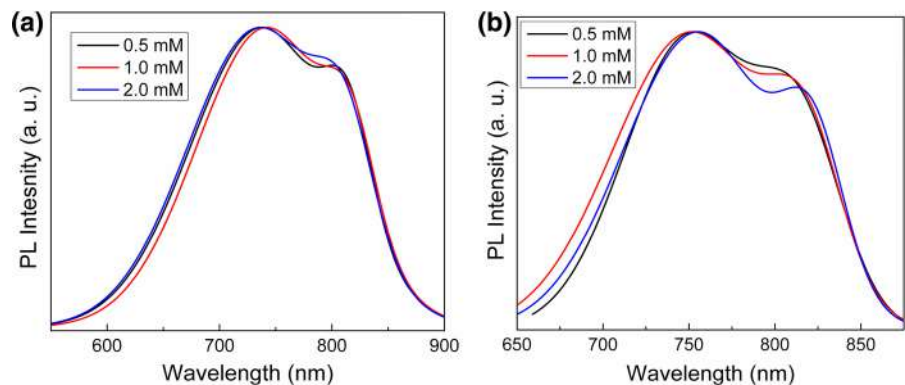


Fig. 8 Cell viability of colo-205 cancer cells determined by trypan blue exclusion test when exposed to TGA-capped CdSe QDs at (a) 10 mM and (b) 15 mM of Se(IV)

cells, whereas the samples at 0.5, 1.0, and 2.0 mM presented an average viability of 89.9, 92.8, and 90.7, respectively. No substantial difference between the experimental and control samples were observed, thus reflecting that the QDs cause a negligible adverse effect against the cellular membrane. The ANOVA test indicated that there is no statistically significant difference attributed to QDs concentrations and excess of selenium in the QDs ($P < 0.05$).

With the emerging use of CdSe QDs as potential nano-probes, it is crucial to understand the cytotoxic effects that can produce the release of Cd ions in unstable nanocrystals toward biological settings. Cd ions are known to have cytotoxic effect when is bonded to the sulphhydryl groups of proteins and the depletion of cellular glutathione levels occurs. Although cadmium (a redox inactive metal) is incapable of directly generating free radicals, it promotes the indirect formation of reactive oxygen species

(ROS), which in turn induce DNA damage, lipid peroxidation, and protein modification (Waisberg et al. 2003). Even though, the mechanism of cadmium's indirect ROS formation is not well understood, it is believed that cadmium can replace iron and cooper in a variety of cytosolic and integral membrane proteins, increasing free iron and copper concentrations, which directly participate in cellular oxidative stress via Fenton reaction. (Hiraishi et al. 1991; Price and Joshi 1983). These reactive oxygen species stimulate the release of cytochrome c that promotes caspase-dependent apoptosis (Petrossillo et al. 2003).

In order to evaluate whether an apoptotic mechanism was activated or not among the cell cultures with a small reduction in viability, the Annexin V assay was performed to determine possible Cd^{+2} -related toxicity in cell cultures using QDs and Cd^{+2} ions at 2.0 mM (Fig. 9). Four groups were systematically measured using a second positive control to generate comparable

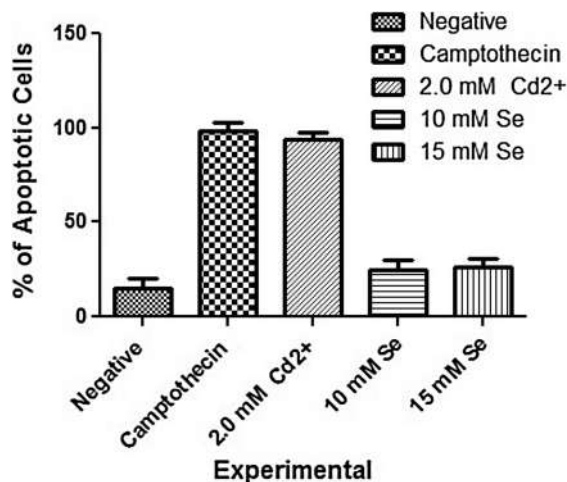


Fig. 9 Annexin V assay tested on TGA-capped CdSe QDs at 10 and 15 mM of Se(IV) showing no apoptosis-induced mechanism and Cd²⁺ as positive control

and reliable results. They show that the percent of apoptotic cells present in the CdSe at 10 mM (average of ~25.0 %) and 15 mM (average of ~26.3 %) is slightly higher than that found in the control (average of ~15.0 %). As expected, the camptothecin positive control shows a large percent of apoptotic cells (average of ~98.0 %), whereas the Cd²⁺ experimental group showed a certain degree of apoptotic activity (average ~96.0 %). The comparison between camptothecin and Cd²⁺ shows the relative apoptotic capability of cadmium ions to be released by the destabilization of the nanocrystal. Both results indicate that there are no abnormal levels of apoptotic cell percentage (less than 10.0 % for 10 mM and 11.3 %

for 15 mM), when compared to the camptothecin and Cd²⁺ group, evidencing that the QDs do not cause apoptosis induction under the testing parameters covered in this study. Taken altogether, the method developed in this study shows that the TGA is an effective biocompatible ligand capable of stabilizing the highly crystalline CdSe QDs, and prevents the toxic emissions of reactive oxygen species that would normally lead to the induction of apoptosis.

Accordingly, both the cell viability and Annexin V assays suggest that the TGA-capped CdSe QDs are non-toxic. To further confirm the biocompatibility of the QDs, study their interaction with the colo-205 human cancer cells, and evaluate their bio-imaging ability, we performed intracellular uptake measurements monitored by confocal microscopy. The cells after 48 h of contact were thoroughly washed and purified with PBS in order to eliminate any excess of QDs adsorbed on the cell membrane. Unfortunately, no detectable emission coming out from the cells was observed, which can be ascribed to the fact that the as-synthesized QDs were uptaken by the cells and that they appear to have a low quantum yield. Varying our synthetic protocol, we synthesized a new set of QDs that can prominently emit light with higher values of quantum yield. Under the same conditions as described above, we observed that the re-suspended cells can emit light more efficiently indicating that the TGA-capped CdSe QDs can penetrate into the live cells without causing cell death, and to be eventually located in the cytosolic regions of cell membrane, consistent with cell viability and Annexin V assays. The fluorescence confocal images of colo-205 cells

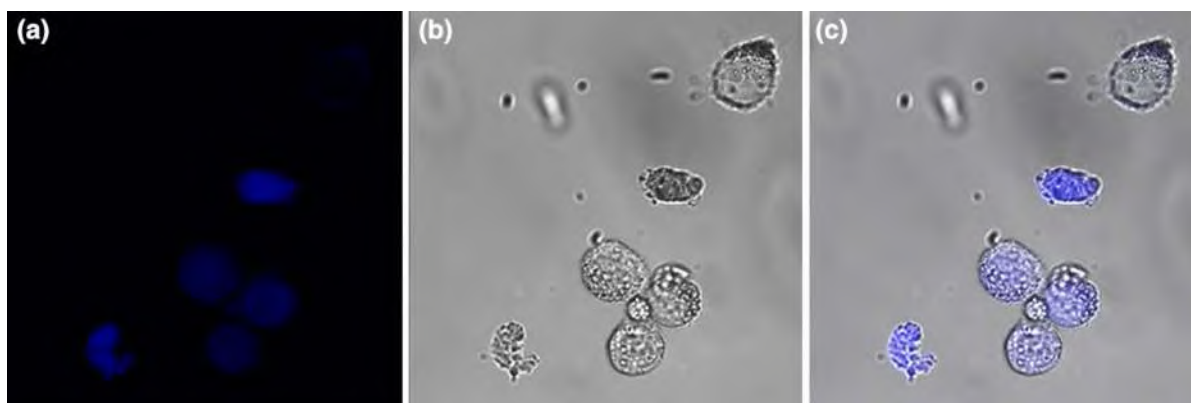


Fig. 10 a–c Fluorescence confocal microscopy images of colo-205 cancer cells when exposed to TGA-capped CdSe QDs at 15 mM of Se(IV) for 48 h. Photos taken at Confocal Imaging Facility at UPR (CIF-UPR)

exposed to the QDs (15 mM) at 2.0 mM with a heating time interval of 20 min are depicted in Fig. 10.

Conclusions

In summary, we have successfully synthesized TGA-capped CdSe QDs directly in water. Our findings indicate that the QDs are non-cytotoxic until a concentration of 2.0 mM, are located within the cytosolic side of cellular membrane, and can be used as bio-imaging agents to efficiently detect colo-205 human cancer cells regardless of the selenium concentration (10 and 15 mM) used for their synthesis. This work brings forth new vistas to further implement the use of water-soluble biocompatible Cd-based QDs for bio-imaging cancer cells, which is critical for the theranostics of the most common cancer types that cause significant mortality over the world population.

Acknowledgments We gratefully acknowledge the financial support of the NSF-REU: Puerto Rico Research Training in Cross-Disciplinary Chemical Sciences (NSF funding CHE 126282). UPR-IFN support under Grant award number, EPS 1002410 is also appreciated. Research reported in this publication was also supported in part by an Institutional Development Award (IDeA) to Dr. Zayas from the National Institute of General Medical Sciences of the National Institutes of Health under grant number P20 GM103475. The content is solely the responsibility of the authors and does not necessarily represent the official views of the National Institutes of Health. We thank Dr. Lymarie Fuentes for her help regarding to fluorescence experiments. J.B-H. thanks PR NASA EPSCoR (NASA Cooperative Agreement NNX13AB22A) for financial support. We thank Bismark Madera for the confocal images taken at CIF-UPR.

References

- Aldeek F, Balan L, Lambert J, Schneider R (2008) The influence of capping thioalkyl acid on the growth and photoluminescence efficiency of CdTe and CdSe quantum dots. *Nanotechnology* 19:475401
- Arslan Z, Ates M, McDuffy W, Agachan MS, Farah IO, Yu WW, Bednar AJ (2011) Probing metabolic stability of CdSe nanoparticles: alkaline extraction of free cadmium from liver and kidney samples of rats exposed to CdSe nanoparticles. *J Hazard Mater* 192:192–199
- Beltran-Huarac J, Wang J, Tanaka H, Jadwisienczak WM, Weiner BR, Morell G (2013) Stability of the Mn photoluminescence in bifunctional ZnS:0.05Mn nanoparticles. *J Appl Phys* 114:053106
- Chan WH, Shiao NH, Lu PZ (2006) CdSe quantum dots induce apoptosis in human neuroblastoma cells via mitochondrial-dependent pathways and inhibition of survival signals. *Toxicol Lett* 167:191–200
- Dailey ME, Mander E, Soll DR, Terasaki M (2006) Confocal microscopy in living cells. In: Pawley JB (ed) *Handbook of biological confocal microscopy*, 3rd edn. Springer, New York, pp 381–413
- Derfus AM, Warren WCM, Bhatia SN (2004) Probing the cytotoxicity of semiconductor quantum dots. *Nano Lett* 4:11–18
- Fang TT, Li X, Wang QS, Zhang ZJ, Liu P, Zhang CC (2012) Toxicity evaluation of CdTe quantum dots with different size on *Escherichia coli*. *Toxicol Vitro* 26:1233–1239
- Gaponik N, Talapin DV, Rogach AL et al (2002) Thiol-capping of CdTe nanocrystals: an alternative to organometallic synthetic routes. *J Phys Chem B* 106:7177–7185
- Hiraishi H, Terano A, Ota S, Mutoh H, Razandi M, Sugimoto T, Ivey KJ (1991) Role for iron in reactive oxygen species-mediated cytotoxicity to cultured rat gastric mucosal cells. *Am J Physiol* 260:G556–G563
- Jaiswal JK, Mattoussi H, Mauro JM, Simon SM (2003) Long-term multiple color imaging of live cells using quantum dot bioconjugates. *Nat Biotechnol* 21:47–51
- Jamieson T, Bakhshi R, Petrova D, Pocock R, Imani M, Seifalian AM (2007) Biological applications of quantum dots. *Biomaterials* 28:4717–4732
- Jayagopal A, Russ PK, Haselton FR (2007) Surface engineering of quantum dots for in vivo vascular imaging. *Bioconjug Chem* 18(1424):1433
- Jiang H, Ju H (2007) Enzyme-quantum dots architecture for highly sensitive electrochemiluminescence biosensing of oxidase substrates. *Chem Commun* 4:404–406
- Kinkeada B, Hegmann T (2009) Effects of size, capping agent, and concentration of CdSe and CdTe quantum dots doped into a nematic liquid crystal on the optical and electro-optic properties of the final colloidal liquid crystal mixture. *J Mater Chem* 20:448–458
- Lewinski NA, Zhu H, Jo H-J et al (2010) Quantification of water solubilized CdSe/ZnS quantum dots in daphnia magna. *Environ Sci Technol* 44:1841–1846
- Lu HY, Shiao NH, Chan WH (2006) CdSe quantum dots induce apoptosis via activation of JNK and PAK2 in human osteoclast cell line. *Med Biol Eng* 26:89–96
- Park Y, Ryu YM, Wang T et al (2014) Spraying quantum dot conjugates in the colon of live animals enabled rapid and multiplex cancer diagnosis using endoscopy. *ACS Nano* 8:8896–8910
- Petrosillo G, Ruggiero FM, Paradies G (2003) Role of reactive oxygen species and cardiolipin in the release of cytochrome c from mitochondria. *FASEB J* 17:2202–2208
- Price DJ, Joshi JG (1983) Ferritin. Binding of beryllium and other divalent metal ions. *J Biol Chem* 258:10873–10880
- Primera-Pedrozo OM, Arslan Z, Rasulev B, Leszczynski J (2012) Room temperature synthesis of PbSe quantum dots in aqueous solution: stabilization by interactions with ligands. *Nanoscale* 4:1312–1320
- Rim SH, Seeff L, Ahmed F, King JB, Coughlin SS (2009) Colorectal cancer incidence in the United States, 1999–2004: an update analysis of data from the national program of cancer registries and the surveillance, epidemiology, and end results program. *Cancer* 115:1967–1976
- Robel I, Subramanian V, Kuno M, Kamat PV (2006) Quantum dot solar cells. Harvesting light energy with CdSe

- nanocrystals molecularly linked to mesoscopic TiO₂ films. *J Am Chem Soc* 128:2385–2393
- Waisberg M, Joseph P, Hale B, Beyersmann D (2003) Molecular and cellular mechanisms of cadmium carcinogenesis. *Toxicology* 192:95–117
- Walling MA, Novak JA, Shepard JR (2009) Quantum dots for live cell and in vivo imaging. *Int J Mol Sci* 10:441–491
- Xue M, Wang X, Wang H, Tang B (2011) The preparation of glutathione-capped CdTe quantum dots and their use in imaging of cells. *Talanta* 83:1680–1686
- Yan M, Zhang Y, Xu K, Fu T, Qin H, Zheng X (2011) An in vitro study of vascular endothelial toxicity of CdTe quantum dots. *Toxicology* 282:94–103
- Yu WW, Qu L, Guo W, Peng X (2003) Experimental determination of the extinction coefficient of CdTe, CdSe, and CdS nanocrystals. *Chem Mater* 15:2854–2860
- Yu WW, Chang E, Drezek R, Colvin VL (2006) Water-soluble quantum dots for biomedical application. *Biochem Biophys Res Commun* 348:781–786
- Zhai C, Zhang H, Du N, Chen B, Huang H, Wu Y, Yang D (2011) One-pot synthesis of biocompatible CdSe/CdS quantum dots and their applications as fluorescent biological labels. *Nanoscale Res Lett* 6:31–35